2018

Effect of mo, nb and v on hot deformation behaviour, microstructure and hardness of microalloyed steels

Navjeet Singh
University of Wollongong, ns106@uowmail.edu.au

Andrii Kostryzhev
University of Wollongong, andrii@uow.edu.au

Chris R. Killmore
BlueScope Steel Limited, Chris.Killmore@bluescopesteel.com

Elena V. Pereloma
University of Wollongong, elenap@uow.edu.au

Effect of mo, nb and v on hot deformation behaviour, microstructure and hardness of microalloyed steels

Abstract

Three novel low carbon microalloyed steels with various additions of Mo, Nb and V were investigated after thermomechanical processing simulations designed to obtain ferrite-bainite microstructure. With the increase in microalloying element additions from the High V-to NbV-to MoNbV-microalloyed steel, the high temperature flow stresses increased. The MoNbV and NbV steels have shown a slightly higher non-recrystallization temperature (1000°C) than the High V steel (975°C) due to the solute drag from Nb and Mo atoms and austenite precipitation of Nb-rich particles. The ambient temperature microstructures of all steels consisted predominantly of polygonal ferrite with a small amount of granular bainite. Precipitation of Nb-and Mo-containing carbonitrides (>20 nm size) was observed in the MoNbV and NbV steels, whereas only coarser (~40 nm) iron carbides were present in the High V steel. Finer grain size and larger granular bainite fraction resulted in a higher hardness of MoNbV steel (293 HV) compared to the NbV (265 HV) and High V (285 HV) steels.

Effect of Mo, Nb and V on hot deformation behaviour, microstructure and hardness of microalloyed steels

Navjeet Singh[1,a*], Andrii G. Kostryzhev[1,b], Chris R. Killmore[2,c], and Elena V. Pereloma[1,3,d]

[1]ARC Research Hub for Australian Steel Manufacturing, University of Wollongong, Wollongong, 2522, Australia

[2]BlueScope Steel Limited, Five Islands Rd, Port Kembla, NSW 2505, Australia

[3]UOW Electron Microscopy Centre, University of Wollongong, NSW 2519, Australia

[a]ns106@uowmail.edu.au, [b] andrii@uow.edu.au, [c] chris.killmore@bluescopesteel.com

[d] elenap@uow.edu.au

Abstract. Three novel low carbon microalloyed steels with various additions of Mo, Nb and V were investigated after thermomechanical processing simulations designed to obtain ferrite-bainite microstructure. With the increase in microalloying element additions from the High V- to NbV- to MoNbV-microalloyed steel, the high temperature flow stresses increased. The MoNbV and NbV steels have shown a slightly higher non-recrystallization temperature (1000°C) than the High V steel (975°C) due to the solute drag from Nb and Mo atoms and austenite precipitation of Nb-rich particles. The ambient temperature microstructures of all steels consisted predominantly of polygonal ferrite with a small amount of granular bainite. Precipitation of Nb- and Mo-containing carbonitrides (>20 nm size) was observed in the MoNbV and NbV steels, whereas only coarser (~40 nm) iron carbides were present in the High V steel. Finer grain size and larger granular bainite fraction resulted in a higher hardness of MoNbV steel (293 HV) compared to the NbV (265 HV) and High V (285 HV) steels.

Introduction

Microalloyed steels containing niobium (Nb), titanium (Ti) and vanadium (V) either added individually or in combination provide an attractive balance between superior strength and good toughness suited for construction industries [1-4]. If the second phase fraction is relatively low, four strengthening mechanisms will operate in microalloyed steels: grain boundary, solid solution, precipitation strengthening and work hardening [1, 5-8]. There is a direct relationship between refinement of ferrite microstructure and condition of austenite (grain size, density of dislocations, deformation bands, and twins) prior to the transformation to ferrite [9-11]. The condition of austenite affects the ferrite nucleation at prior austenite grain boundaries and other defects in the austenite matrix. Alloying elements play a vital role in refining the austenite grain size and accumulation of defects in the matrix by retarding restoration processes such as recovery and recrystallization. Nb and Mo are the most effective elements among other alloying elements that obstruct the restoration processes, whether they are in the form of solute atoms and/or carbonitride particles (e.g. Nb (C, N)) [12-17]. Thus, in microalloyed steels it is necessary to examine the high temperature stress-strain behaviour to understand the state of austenite prior to its transformation to ferrite. The objectives of this paper were to investigate the effects of microalloying elements additions on (i) hot flow behavior, (ii) non-recrystallization (T_{nr}), austenite to ferrite start (A_3) and finish (A_1) temperatures, and (iii) ambient temperature microstructure and hardness.

Materials and experimental techniques

Three microalloyed steels (Table 1) designated as MoNbV (containing increased Nb and Mo), NbV (increased Nb and decreased Mo) and High V (increased V) steels were melted in a 60 kg induction furnace and cast as $75 \times 100 \times 150$ mm blocks by Hycast Metals Pty, Sydney. The blocks were homogenised at 1250 °C for 30 h, to equalize chemical composition, then forged at Granger Forge & Engineering, Sydney, in the temperature range of 1250-900 °C along the 100 mm side to 28 mm plate thickness, to assure 3.5 times reduction of the as-cast microstructure. The forged plates were cut into standard $20 \times 15 \times 10$ mm Gleeble samples. Multi-hit compression tests were carried out using Gleeble 3500 thermomechanical simulator to determine T_{nr}, A_3 and A_1 temperatures according to the schedule presented in Fig. 1a. Constant strain of 0.1 at strain rate of 5 s^{-1} was applied in each deformation cycle. The mean flow stress (MFS) in each deformation cycle was calculated using Eq. 1 [18].

$$\text{MFS} = \frac{1}{\varepsilon_b - \varepsilon_a} \int_{\varepsilon_a}^{\varepsilon_b} \sigma d\varepsilon \qquad (1)$$

where ε_a and ε_b are the lower and upper strain values in a particular pass and σ is the stress in this pass. T_{nr}, A_3 and A_1 temperatures were determined using points of substantial MFS deviation on the MFS vs inverse temperature graphs (Fig. 1b).

Table 1 Chemical composition of the steels investigated (wt. %).

Steels	C	Mn	Si	Al	Cr	Ni	N	Σ (Mo, Nb, V)
MoNbV	0.054	1.47	0.26	0.003	0.31	0.23	0.0133	0.381
NbV	0.082	1.52	0.29	0.003	0.52	0.21	0.013	0.181
High V	0.110	1.39	0.26	0.003	0.51	0.011	0.0129	0.213

Based on T_{nr} and A_3 temperatures of the steels investigated, four pass thermomechanical processing schedule (TMP) was designed (Fig. 1c). For the analysis of high temperature stress-strain behavior, the hot stress-strain curves were approximated by a 9th order polynomial fit. After TMP, the samples were cut perpendicular to the transverse direction (TD), then polished and etched using 2% Nital solution. The microstructures were examined in the mid-thickness position between the compression anvils using field emission gun scanning electron microscope JEOL JSM-7001F. Secondary electron images were taken at 15 kV of accelerating voltage, while the particle analysis was carried out at 6 kV of accelerating voltage (to reduce the beam-matrix interaction volume and improve the accuracy of chemical analysis). Vickers hardness was measured using a Struers Emco-Test DuraScan-70 hardness tester applying 0.5 kgf load.
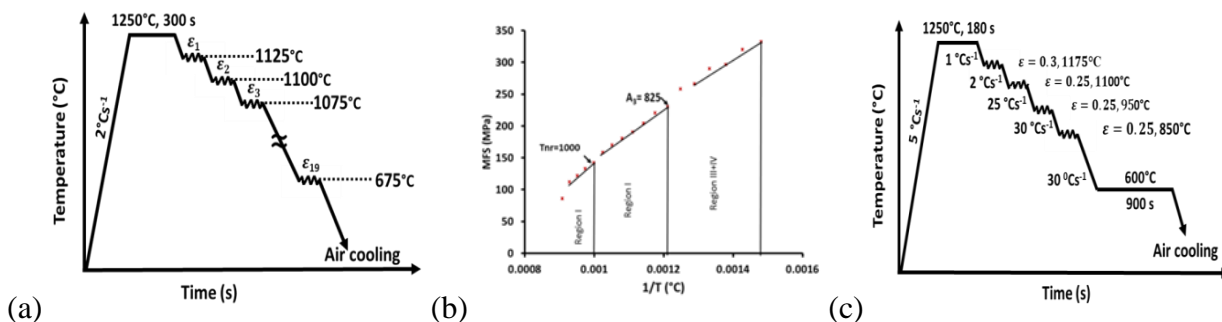

Figure 1. (a) Scheme of the multi-hit compression schedule, (b) MFS vs inverse temperature graph for MoNbV steel, and (c) scheme of the main 4-stage processing schedule.

Results and discussion

Hot deformation behavior

Multi-hit compression tests (Fig. 1a) have shown T_{nr} in the MoNbV and NbV steels being 25 °C higher compared to the High V steel (Table 2). This resulted from a higher Mo and Nb contents in MoNbV and NbV steels. Both Mo and Nb retard recrystallization either by solute drag effect or by precipitates [19], such as (Nb,Mo)(C,N) and Nb(C,N) found in MoNbV and NbV steels. In order to evaluate the effect of steel composition on hot deformation behavior of steels, equivalent stress-

strain curves at 1100 °C, 950 °C and 850 °C were plotted (Figs. 2a-c). In all studied conditions, the stress at first increased with increasing strain, due to work hardening. After reaching a peak, the stress decreased with increasing strain due to softening. With an increase in Nb and Mo contents, the peak stress values increased for all set temperatures due to increased solid solution and precipitation strengthening contributions (Table 2). With a decrease in deformation temperature, the stress-strain curves moved upwards along the stress axis and the Young's modulus for all the steels increased from about 2.3 GPa at 1100 °C to 4.6 GPa at 950 °C and to 9.0 GPa at 850 °C due to slower recovery of sub-structure.

Table 2. Hot deformation characteristics of the steels investigated (σ are given in MPa).

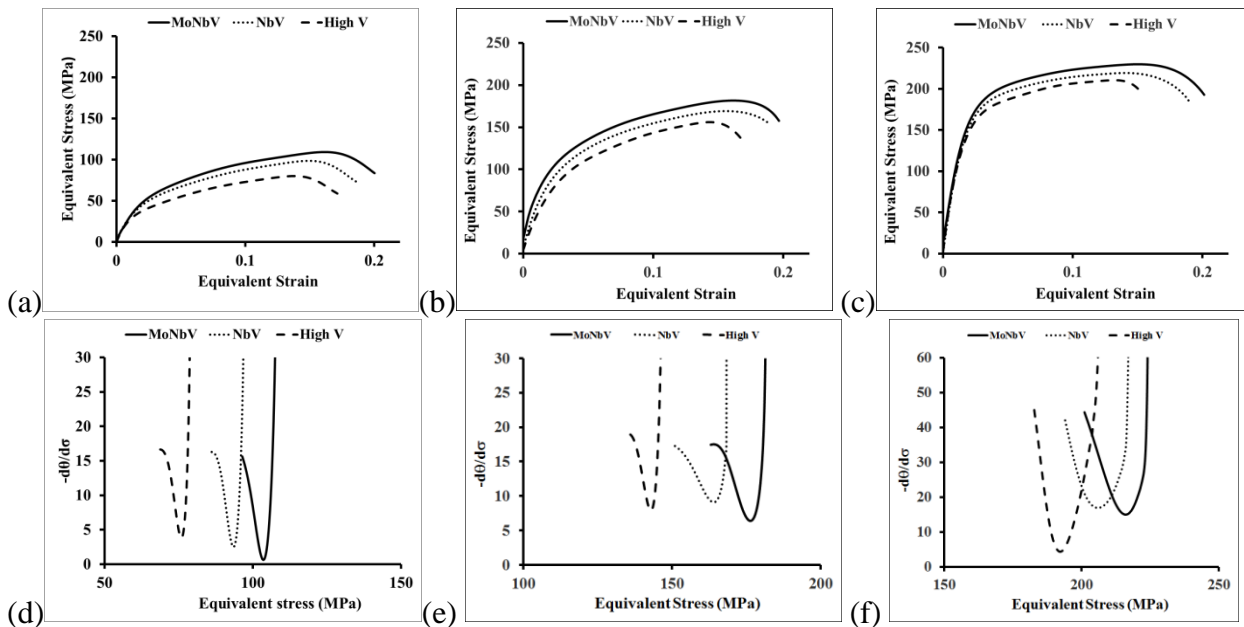| Steels | T_{nr}, °C | A_3, °C | A_1, °C | Dynamic recrystallization | | | | | | Dynamic transformation | | |
| | | | | 1100 °C | | | 950 °C | | | 850 °C | | |
				ε_c	σ_c	σ_{peak}	ε_c	σ_c	σ_{peak}	ε_c	σ_c	σ_{peak}
MoNbV	1000	825	775	0.13	104	109	0.13	176	182	0.08	216	230
NbV	1000	875	775	0.12	94	99	0.13	164	170	0.08	209	219
High V	975	850	725	0.11	76	80	0.11	142	156	0.06	193	210

Figure 2. Equivalent stress-strain curves at (a) 1100 °C, (b) 950 °C, and (c) 850 °C and double derivative vs equivalent stress curves at (d) 1100 °C, (e) 950 °C and (f) 850 °C.

In order to study the softening phenomenon, the double differentiation method [20] was employed. For all studied temperatures, the $-(d\theta/d\sigma)$ vs σ curves showed one minima (Fig. 2d-f). These minima points, indicating the onset of dynamic recrystallization (DRX) at 1100 to 950 °C and dynamic transformation to ferrite (DT) at 850 °C, were used to determine the critical stress (σ_c). Corresponding critical strain (ε_c) was obtained from Figs. 2a-c. With an increase in microalloying, ε_c and σ_c of DRX increased (Table 2), which is in line with the effects of Mo and Nb atoms and precipitates on retardation of recovery and recrystallization. For each steel, the critical stress for DRX increased with the temperature decrease from 1100 to 950 °C. The DRX was not completed at either temperature as there is no characteristic stress plateau present on the curves (Figs. 2a-c). However, metadynamic recrystallization could have taken place during the cooling after deformation at 1100 °C. Although the A_3 temperature for MoNbV steel is 25 °C below the deformation temperature of 850 °C, the occurrence of DT at the temperatures well above the ortho-equilibrium temperature (A_{e3}) was observed previously [21-23]. It is known that, alloying elements such as Mo, Mn, Nb, V and Cr are profoundly involved in restraining DT of ferrite. Alloying elements segregate to austenite grain boundaries and reduce their energy - as a result,

transformation driving force for DT decreases [24]. However, Nb can exhibit opposite effects on DT depending on its state. In solution, Nb decreases DT in the same way as other elements do, by segregating to austenite grain boundaries. Precipitation of Nb as (Nb,Mo)(C,N) and (Nb)(C,N) lowers the content of Nb, Mo, C and N in solution [25]. Consequently, the transformation driving force for DT increases [24].

Ambient temperature microstructure and hardness

Figure 3 shows the SEM micrographs of the steels investigated. After coiling at 600°C for 900 s, the microstructure in all steels consisted of polygonal ferrite (PF) and a fraction of granular bainite (GB). The ferrite grain size distribution was bimodal in all steels. Two ferrite size ranges were identified: <5 μm and >5 μm (Table 3). In each range, the average ferrite grain size was smaller in the MoNbV and NbV steels, compared to the High V steel. This might originate from a smaller prior austenite grain size in the Mo- and Nb-microalloyed steels related to the effect of solute atoms and precipitates on the retardation of austenite grain growth in these steels. Inhomogeneity of ferrite microstructures could arise from three major causes: (i) bimodal prior austenite microstructure following partial DRX, (ii) non-uniform distribution of Nb and Mo solute atoms and their precipitates, (Nb,Mo)(C,N) in MoNbV steel and (Nb)(C,N) in NbV steel; and (iii) partial dynamic transformation of austenite to ferrite. The GB area fraction increased with microalloying (Table 3). This can be explained by increased hardenability in Mo [26, 27] and Nb [19, 28] containing steels.
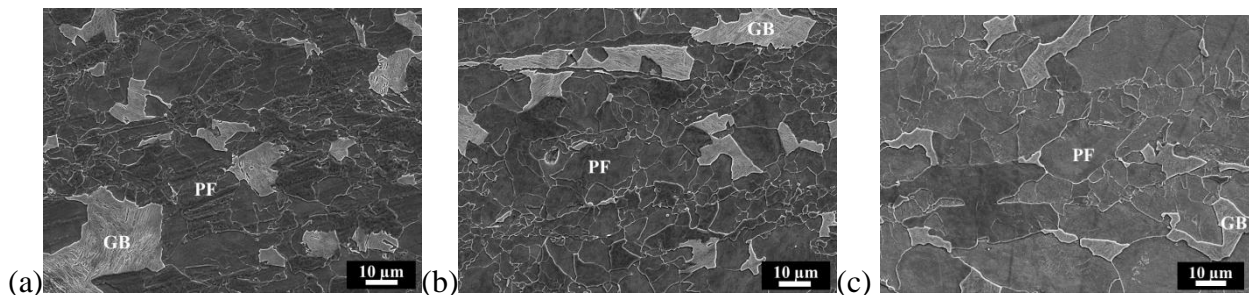

Figure 3. SEM images of microstructure of (a) MoNbV (b) NbV and (c) High V steels: PF – polygonal ferrite, GB – granular bainite.

Table 3 Microstructural parameters for the steels investigated.

Steels	Average ferrite grain size, μm		Second phase fraction, %	Particles		Hardness, HV
	<5 μm range	>5 μm range		size, nm	number density, μm^{-2}	
MoNbV	2 ± 1	8 ± 2	14 ± 5	25 ± 6	0.8 ± 0.2	293±11
NbV	2 ± 1	8 ± 2	11 ± 3	28 ± 10	1.3 ± 0.84	265±8
High V	3 ± 1	10 ± 5	9 ± 2	40 ± 13	0.5 ± 0.1	285±10

Particle precipitation was studied using SEM imaging and EDS (Figure 4). In accordance with steel compositions, (Nb,Mo)(C,N) particles were observed in the MoNbV steel, Nb(C,N) in the NbV steel and Fe_3C in the High V steel. Based on the particle sizes (Table 3), these precipitates presumably formed in austenite, possibly at ~950 °C or lower, thus restricting DRX of austenite and assisting the DT of ferrite at 850 °C. The presence of Mo in the MoNbV steel increased Nb solubility in austenite, which could refine the (Nb,Mo)(C, N) precipitates and reduce their number density with respect to the NbV steel (compare 25±6 nm and 28 ± 10 nm of average particles size in the MoNbV and NbV steels, respectively; 0.8 ± 0.2 μm^{-2} and 1.3 ± 0.84 μm^{-2} of particles number density in the MoNbV and NbV steels, respectively, Table 3). Absence of Mo and Nb solute atoms and precipitates in the High V steel had to favor DRX of austenite and DT to ferrite. This can be supported by lower critical strains and stresses of DRX and DT in the High V steel (Table 2).

The MoNbV steel has shown the highest hardness of 293 HV, NbV steel with the lowest (265 HV), and High V steel an intermediate value (285 HV). The highest MoNbV steel hardness could originate from the largest GB fraction and a higher solid solution strengthening from Mo and

Nb atoms. The relatively high hardness of the High V steel can be related to the high density of random and interphase V-rich precipitates. These were not observed with SEM, but were evident from scanning transmission electron microscopy and atom probe tomography studies of this steel after a slightly different TMP schedule. Further investigation is required for this condition.
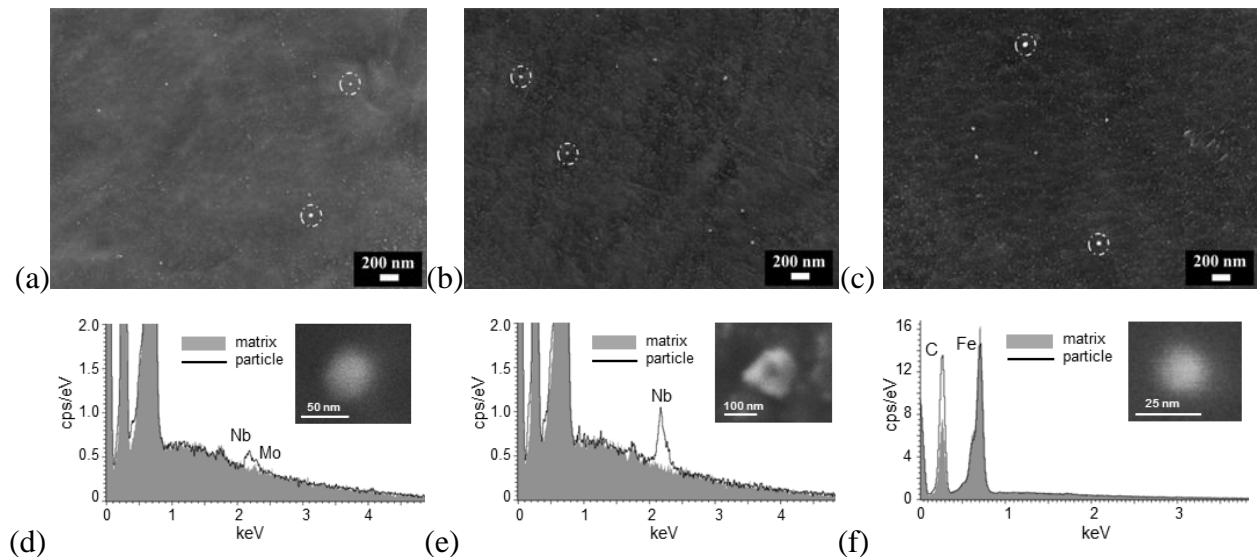

Figure 4. (a-c) SEM images of precipitates and EDS spectra of (d) (Nb,Mo)(C,N) particle in MoNbV steel, (e) Nb(C,N) in NbV steel, and (f) Fe_3C in High V steel.

Summary

The investigation of newly developed Mo, Nb and V microalloyed steels has shown that Mo and Nb additions increase the non-recrystallization temperature and critical stresses and strains for onset of dynamic recrystallization. The hot deformation stresses increase with Mo and Nb additions in the deformation temperature range of $1100 - 850$ °C. This is related to strong solute drag and particle pinning effects of Mo and Nb. The ambient temperature microstructures of all three steels consisted of polygonal ferrite and granular bainite. The bainite area fraction increased with Nb and Mo additions due to the effect of these elements on hardenability. Finer grain size and larger bainite fraction resulted in a higher hardness of MoNbV steel (293 HV) compared to other steels.

References

[1] X. Chen, Y. Huang, Hot deformation behavior of HSLA steel Q690 and phase transformation during compression. J. Alloy Compd. 619 (2015) 564-571.

[2] X. Kong, et al., Optimization of mechanical properties of high strength bainitic steel using thermo-mechanical control and accelerated cooling process, J. Mater. Process. Tech. 217 (2015) 202-210.

[3] G.W. Yang, et al., Ultrafine grained austenite in a low carbon vanadium microalloyed steel, J. Iron Steel Res. Int. 20(4) (2013) 64-69.

[4] D.B. Park, et al., Strengthening mechanism of hot rolled Ti and Nb microalloyed HSLA steels containing Mo and W with various coiling temperature, Mater. Sci. Eng. A 560 (2013) 528-534.

[5] C.Y. Chen, et al., Precipitation hardening of high-strength low-alloy steels by nanometer-sized carbides, Mater. Sci. Eng. A 499(1-2) (2009) 162-166.

[6] Y.F. Shen, C.M. Wang, X. Sun, A micro-alloyed ferritic steel strengthened by nanoscale precipitates, Mater. Sci. Eng. A 528(28) (2011) 8150-8156.

[7] M. Cabibbo, et al., Effect of thermo-mechanical treatments on the microstructure of micro-alloyed low-carbon steels, J. Mater. Sci. 43(21) (2008) 6857-6865.

[8] A.G. Kostryzhev, O.O. Marenych, C.R. Killmore, E.V. Pereloma, Strengthening mechanisms in thermomechanically processed NbTi-microalloyed steel, Metal. Mater. Trans. A 46(8)(2015)3470-3480.

[9] Y. H. Bae, J. S. Lee, J.-K. Choi, W.-Y. Choo, S. H. Hong, Effects of austenite conditioning on austenite/ferrite phase transformation of HSLA steel, Mater. Trans. 45(1) (2004) 137-142.

[10] R. Kaspar, U. Lotter, C. Biegus, The influence of thermomechanical treatment on the transformation behaviour of steels, Steel Res. Int. 65 (1994) 242–247.

[11] M.-C. Zhao, K. Yang, F.-R. Xiao, Y.-Y. Shan, Continuous cooling transformation of undeformed and deformed low carbon pipeline steels, Mater. Sci. Eng. A 355 (2003) 126-136.

[12] W. P. Sun, M. Militzer, D. Q. Bai, J. J. Jonas, The effects of precipitation on recrystallization under multipass deformation conditions, Acta Metal. Mater. 41(12) (1993) 3595-3604.

[13] Z.H. Zhang, et al., The effect of Nb on recrystallization behavior of a Nb micro-alloyed steel. Mater. Sci. Eng. A 474(1-2) (2008) 254-260.

[14] S. Vervynckt, K. Verbeken, P. Thibaux, M Liebeherr, Y. Houbaert, Austenite recrystallization–precipitation interaction in niobium microalloyed steels, ISIJ Int. 49(6) (2009) 911–920.

[15] M. G Akben, B. Bacroix, J.J. Jonas, Effect of vanadium and molybdenum addition on high temperature recovery, recrystallization and precipitation behaviour of niobium-based microalloyed steels, Acta Metal. 31 (1983) 161-174.

[16] H.L. Andrade, M.G. Akben, J.J. Jonas, Effect of molybdenum, niobium, and vanadium on static recovery and recrystallization and on solute strengthening in microalloyed steels, Metal. Trans. A 14(10) (1983) 1967–1977.

[17] T. Schambron, L. Chen, T. Gooch, A. Dehghan-Manshadi, E.V. Pereloma, Effect of Mo concentration on dynamic recrystallization behavior of low carbon microalloyed Steels, Steel Res. Int. 84(12) (2013) 1191-1195.

[18] J.F. Siciliano, et al., Mathematical modeling of the mean flow stress, fractional softening and grain size during the hot strip rolling of C-Mn steels, ISIJ Int. 36(12) (1996) 1500-1506.

[19] Y. Chen, D. Zhang, Y. Liu, H. Li, D. Xu, Effect of dissolution and precipitation of Nb on the formation of acicular ferrite/bainite ferrite in low-carbon HSLA steels. Mater. Charact. 84(2013)232-239.

[20] N. Khodaie, D.G. Ivey, H. Henein, Extending an empirical and a fundamental bainite start model to a continuously cooled microalloyed steel, Mater. Sci. Eng. A 650 (2016) 510-522.

[21] H. Yada, Y. Matsumura, T. Senuma, Proc. 1st Conf. Physical Metallurgy of Thermomechanical Processing of Steels and Other Metals (THERMEC-88), ed. by I. Tamura, ISIJ, Tokyo, 1988, 200.

[22] J. J. Jonas, C. Ghosh, V. V. Basabe, Effect of dynamic transformation on the mean flow stress, Steel Res. Int. 84(3) (2013) 253-258.

[23] C. Ghosh, V. V. Basabe, J. J. Jonas, Determination of the critical strains for the initiation of dynamic transformation and dynamic recrystallization in four steels of increasing carbon contents, Steel Res. Int. 84 (2013) 490-494.

[24] S. Zajac, B. Jansson, Thermodynamics of the Fe-Nb-CN system and the solubility of niobium carbonitrides in austenite, Metal. Mater. Trans. B 29(1) (1998) 163-176.

[25] K. Junhua, et al., Influence of Mo content on microstructure and mechanical properties of high strength pipeline steel, Mater Des. 25(8) (2004) 723-728.

[26] H.I. Aaronson, W.T. Reynolds Jr., G.R. Purdy, The incomplete transformation phenomenon in steel, Metal. Mater. Trans. A 37 (2006) 1731-1745.

[27] J. Kong, C. Xie, Effect of molybdenum on continuous cooling bainite transformation of low-carbon microalloyed steel, Mater. Des. 27 (2006) 1169–1173.

[28] Y.-K. Lee, J.-M. Hong, C.-S. Choi, J.-K. Lee, Continuous cooling transformation temperatures and microstructures of niobium bearing microalloyed steels, Mater. Sci. Forum 475-479(2005) 65-68.